

Isomeric Cross Sections and Yield Ratios of (d,p) Reactions below 15 MeV*

J. B. NATOWITZ† AND R. L. WOLKE

Wherrett Laboratory of Nuclear Chemistry, University of Pittsburgh, Pittsburgh, Pennsylvania

(Received 5 October 1966)

Absolute cross sections and isomeric yield ratios of (d,p) reactions in Co^{60} , Y^{89} , Rh^{103} , Pd^{110} , Cd^{114} , Cs^{133} , Ta^{181} , Re^{187} , and Pt^{196} have been determined between ~ 4 and ~ 15 MeV. The isomer ratios are found to increase gradually with bombarding energy from values at lower energies which are only slightly greater than the ratios for the production of the same isomeric pairs by the (n,γ) reaction. The qualitative features of (d,p) isomer ratios are discussed. Isomer ratios have been calculated at 15 MeV for seven (d,p) reactions in even-even targets by using distorted-wave Born approximation to obtain the initial angular-momentum distributions and computing the effects of subsequent gamma-ray cascades leading to the observed isomeric states. Agreement with experiment of the order of 15–20% is achieved. The effects of various cascade treatments on the agreement of the calculated isomer ratios with experiment are discussed.

I. INTRODUCTION

THE fact that certain nuclides can be produced as nuclear reaction products in two relatively long-lasting and independently observable isomeric states, differing substantially in total angular momentum but only slightly in energy, has provided an opportunity for the radiochemical study of the role of angular momentum in nuclear reactions. A large number of isomer yield ratios (or isomer ratios), σ_H/σ_L , where σ_H and σ_L are the cross sections for the production of the high-spin and low-spin isomers of the residual nucleus, respectively, have accordingly been determined. These have been compiled by Wing.¹ Although the interpretation of isomer-ratio data is usually hindered by a lack of detailed structural knowledge and by the complicated energy and spin redistributions which take place before the final isomeric states can be observed radiochemically, analyses of both the absolute values and the energy dependences of isomer ratios have been of value, leading, for example, to information about the spin dependence of nuclear level densities.^{2–4}

Except for some calculations of isomer ratios in high-energy knock-on reactions,⁵ the quantitative interpretation of isomer-ratio data has until now been limited to reactions which appear to take place by the compound-nucleus mechanism, statistical methods being employed to calculate the spin distributions resulting from the capture, evaporation, and de-excitation processes. While a few (d,p) isomer ratios^{6–11} have been reported and

qualitatively discussed, there has as yet been no attempt at the quantitative calculation of isomer ratios for these reactions, which are known to take place primarily by a direct-interaction mechanism.

In view of the success of modern stripping theory in explaining certain aspects of (d,p) reactions at moderate energies, it was thought appropriate to subject some of the current concepts of stripping and nuclear structure to the test of predicting the magnitudes of (d,p) isomer ratios. Accordingly, several (d,p) isomer ratios have been measured in the present work, with the dual objectives of seeking any systematic behavior which might be characteristic of the stripping process and of attempting to calculate the measured ratios from theory. Absolute cross sections and isomer ratios were obtained radiochemically by the stacked-foil technique for nine (d,p) reactions as a function of deuteron energy from ~ 4 to ~ 15 MeV.

II. EXPERIMENTAL PROCEDURE

Metal foils were used as targets whenever possible. If foils were unavailable, uniform ($\pm 4\%$) layers of powdered compounds were deposited on backings of glass-fiber filter paper, weighed, covered with Mylar tape, and assembled into stacks with Al foils as beam degraders. The details of the preparation of powdered targets and the calculation of deuteron energy degradation in the stacks have been described elsewhere.¹²

The target stacks were irradiated in a scattering chamber at the University of Pittsburgh cyclotron. Behind the target stack, a Faraday cup connected to a

* Work supported in part by the U. S. Atomic Energy Commission.

† Present address: Department of Chemistry, State University of New York, Stony Brook, New York.

¹ J. Wing, Argonne National Laboratory Report No. ANL 6598, 1962 (unpublished).

² R. Vandenbosch and J. R. Huizenga, *Phys. Rev.* **120**, 1313 (1960).

³ C. T. Bishop, J. R. Huizenga, and J. P. Hummel, *Phys. Rev.* **135**, B401 (1964).

⁴ D. W. Seegmiller, University of California Radiation Laboratory Report No. UCRL 10850, 1963 (unpublished).

⁵ N. T. Porile and S. Tanaka, *Phys. Rev.* **130**, 1541 (1963); I. Levenberg *et al.*, *Nucl. Phys.* **51**, 673 (1964).

⁶ J. R. Huizenga and R. Vandenbosch, *Phys. Rev.* **120**, 1305 (1960).

⁷ A. W. Fairhall, U. S. Atomic Energy Commission Report No. 2128, 1952 (unpublished).

⁸ R. A. Sharp and A. C. Pappas, *J. Inorg. Nucl. Chem.* **10**, 173 (1959).

⁹ L. J. Gilly, G. A. Henriot, M. Preciosa Alves, and P. C. Capron, *Phys. Rev.* **131**, 1727 (1963); K. I. Zherebtsova *et al.*, *Zh. Eksperim. i Teor. Fiz.* **35**, 1355 (1959) [English transl.: *Soviet Phys.—JETP* **8**, 947 (1959)].

¹⁰ C. Riley and B. Linder, *Phys. Rev.* **134**, B559 (1964).

¹¹ S. J. Nassiff, A. Mocoora, and H. Vignau, Argentinian National Atomic Energy Commission Report No. 99, 1963 (unpublished).

¹² J. B. Natowitz, F. Pement, and R. L. Wolke, *Rev. Sci. Instr.* **37**, 121 (1966).

strip-chart recorder provided a record of beam-intensity fluctuations during the irradiations. Because the deuterons were scattered extensively in the thick stacks, however, the integrated incident beam current was determined independently after the irradiation by 4π -counting the β activity induced in a Ta foil which headed each stack. The Ta-foil monitors were calibrated against the Faraday cup under conditions of negligible scattering. Irradiations of Ta foils with deuterons of energies from 14.3 to 14.9 MeV showed that the β activation cross section was constant to less than 1%, showing that the monitoring method was insensitive to cyclotron energy fluctuations.

After the irradiations, the targets were subjected to adaptations of standard radiochemical procedures.¹³ The final samples were mounted either on Al cards and covered with 0.9 mg/cm² of Mylar or between two films of aluminized Mylar on an aluminum ring. Absolute β or γ counting was accomplished with calibrated end-window or 4π methane-flow proportional counters or with a calibrated 3 in. \times 3 in. NaI(Tl) crystal and a 512-channel pulse-height analyzer.

Aspects of the individual experiments which deserve special comment are noted in the Appendix. Unless otherwise stated, decay schemes from Ref. 14 were employed. When experimental internal conversion coefficients were unavailable, the calculated coefficients of Rose¹⁵ were used.

The numbers of metastable and ground-state product nuclei N_m^0 and N_g^0 present at the end of the irradiation were computed from the measured activities by utilizing the appropriate detection efficiencies, decay-scheme data, absorber corrections, and chemical yields. A simplification arises if the metastable state is longer lived than the ground state, as in two of the cases studied in the present work. After a few ground-state half-lives, the isomers are in equilibrium, and both decay with the half-life of the metastable state. Under these conditions, the number of metastable nuclei at the end of the irradiation is given by

$$N_m^0 = (-dN_g/dt)(\lambda_g - \lambda_m) / f_{mg}\lambda_m\lambda_g e^{-\lambda_m t}, \quad (1)$$

where $-dN_g/dt$ is the ground-state disintegration rate at any time t after equilibrium has been established, measured from the end of the irradiation, and f_{mg} is the fraction of metastable-state disintegrations which lead to the ground state. The amounts of both isomers are thus determined by counting only the ground-state radiations; errors in detection efficiencies are therefore eliminated from the cross-section ratio.

¹³ Subcommittee on Radiochemistry, *Radiochemistry Monograph Series NAS-NS* (National Academy of Sciences—National Research Council, Washington, D. C.).

¹⁴ *Nuclear Data Sheets*, compiled by K. Way *et al.* (Printing and Publishing Office, National Academy of Sciences—National Research Council, Washington 25, D. C.).

¹⁵ M. E. Rose, *Internal Conversion Coefficients* (North-Holland Publishing Company, Amsterdam, 1958).

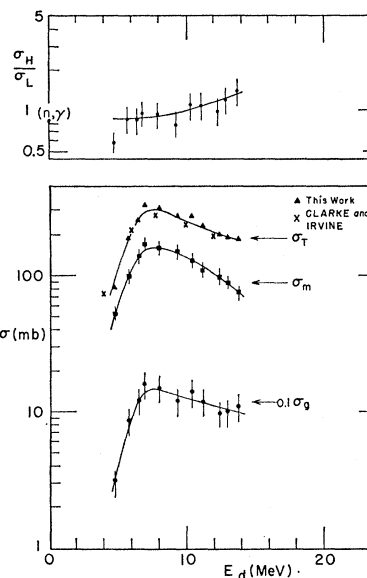


FIG. 1. Absolute cross sections and isomeric yield ratios of the reaction $\text{Co}^{59}(d,p)\text{Co}^{60m,g}$. The (n,γ) isomer ratio is from B. Keisch, *Phys. Rev.* **129**, 769 (1963). Also shown are total cross sections measured by Clarke and Irvine (reported in Ref. 18).

The individual cross sections σ_m and σ_g can then be computed from N_m^0 and N_g^0 through the usual secular-equilibrium relation, beam-intensity fluctuations having been of short periods as compared with the mean lifetimes of the products. In most cases, however, the ratio of the cross sections was obtained directly from the equation¹⁶

$$\frac{\sigma_g}{\sigma_m} = \frac{N_g^0 \lambda_g Q_m}{N_m^0 \lambda_m Q_g} \frac{f_{mg} \lambda_m}{\lambda_g - \lambda_m} \left(\frac{\lambda_g Q_m}{\lambda_m Q_g} - 1 \right), \quad (2)$$

where Q is the saturation factor $1 - e^{-\lambda T}$ achieved by an irradiation of duration T . The cross-section ratio arrived at by the use of this equation is independent of target uniformity, beam intensity, and chemical yield.

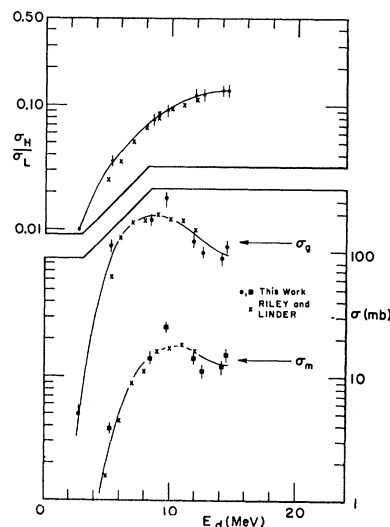


FIG. 2. Absolute cross sections and isomeric yield ratios of the reaction $\text{Y}^{89}(d,p)\text{Y}^{90m,g}$. Also shown are the data of Riley and Linder (Ref. 10).

¹⁶ This equation is analogous to those given by Wing (Ref. 1) and S. Iwata, *J. Phys. Soc. Japan* **17**, 1323 (1962).

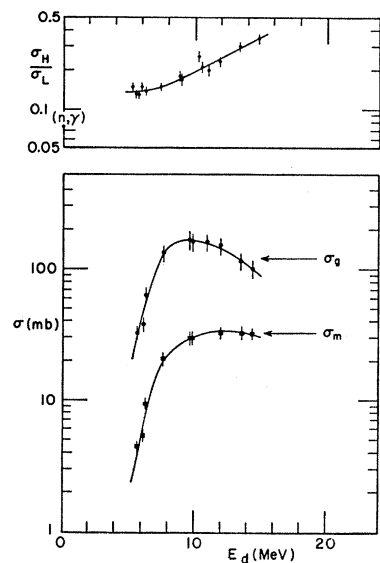


FIG. 3. Absolute cross sections and isomeric yield ratios of the reaction $\text{Rh}^{108}(d,p)\text{-Rh}^{104m,g}$. The (n,γ) isomer ratio is from B. Keisch, Phys. Rev. **129**, 769 (1963).

III. EXPERIMENTAL RESULTS

A. Correlations

The absolute cross sections and isomer ratios measured in the present work are plotted as functions of deuteron energy in Figs. 1-9. The experimental errors shown in the figures were obtained by assigning estimated errors to all measured quantities and propagating

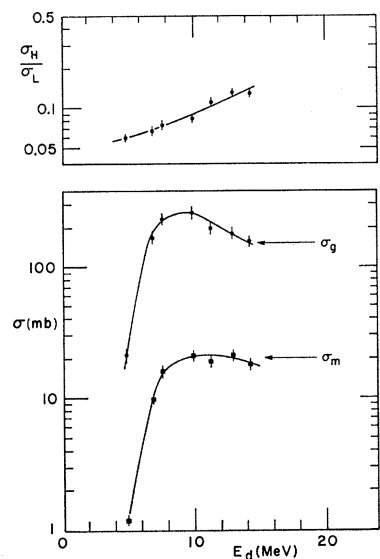


FIG. 4. Absolute cross sections and isomeric yield ratios of the reaction $\text{Pd}^{110}(d,p)\text{-Pd}^{111m,g}$.

them through the computations according to statistical laws.

The measured isomer ratios range over two orders of magnitude but are all similar in shape, increasing slowly with energy except for $\text{Y}^{90m,g}$ and $\text{Ta}^{182m,g}$, whose ratios rise rather steeply. As previously noted,¹⁰ a slowly increasing isomer ratio is usually to be expected in direct

interactions in which only a fraction of the projectile's angular momentum is transferred to the target nucleus. It has also been noted¹⁰ that since the $7+$ metastable state of Y^{90} corresponds to the excitation of a proton, it is not initially populated in a simple (d,p) reaction, but must be formed by the decay of higher-energy levels which must also have relatively high angular momenta.

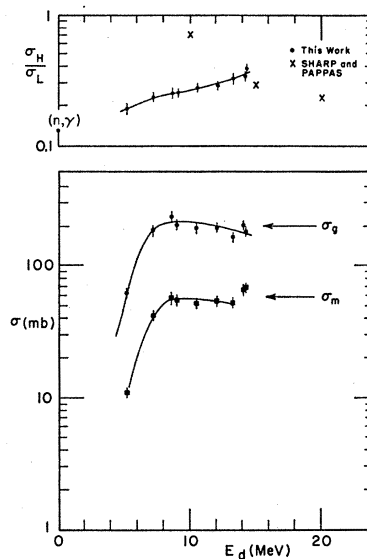


FIG. 5. Absolute cross sections and isomeric yield ratios of the reaction $\text{Cd}^{114}(d,p)\text{-Cd}^{115m,g}$. The (n,γ) isomer ratio is from A. C. Wahl and N. A. Bonner, Phys. Rev. **85**, 570 (1952). Also shown are the (d,p) isomer ratios reported by Sharp and Pappas (Ref. 8).

This may account for the low values of the $\text{Y}^{90m,g}$ ratio at lower energies, and hence for its steeper rise. Indications¹⁷ are that the metastable state of Ta^{182} is $8+$, $9+$, or $10+$. If the spin is indeed as high as 9 or 10, this state also would not be populated in a simple (d,p) reaction without core excitation, and the isomer ratio would be small at lower energies.

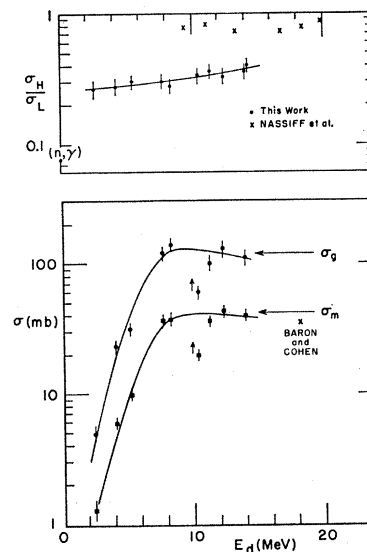


FIG. 6. Absolute cross sections and isomeric yield ratios of the reaction $\text{Cs}^{133}(d,p)\text{-Cs}^{134m,g}$. The (n,γ) isomer ratio is from Ref. 17. Also shown are the (d,p) isomer ratio data of Nassiff *et al.* (Ref. 11) and a value of σ_m at ~ 18 MeV reported by N. Baron and B. L. Cohen, Phys. Rev. **129**, 2636 (1963).

¹⁷ A. W. Sunyar and P. Axel, Phys. Rev. **121**, 1158 (1961).

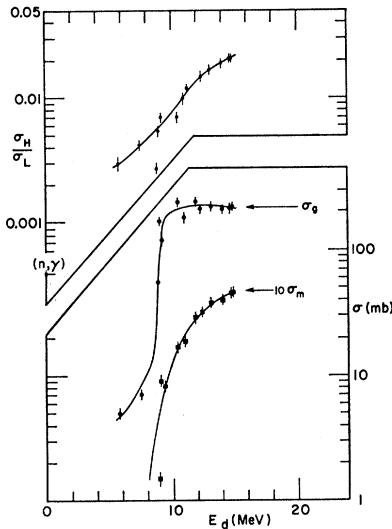


FIG. 7. Absolute cross sections and isomeric yield ratios of the reaction $Ta^{181}(d,p)-Ta^{182m,g}$. The (n,γ) isomer ratio is from Ref. 17.

Certain of the present data can be compared with previous measurements. The total (d,p) cross section $\sigma_m + \sigma_g$ for the production of Co^{60} , shown in Fig. 1, is in good agreement with the data of Clark and Irvine as reported by Peaslee.¹⁸ The Y^{90} excitation functions and isomer ratios shown in Fig. 2 are in agreement with those recently obtained by Riley and Linder,¹⁰ who used evaporated rather than powdered targets, and who

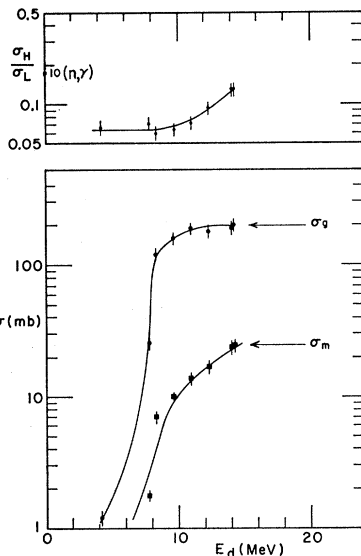


FIG. 8. Absolute cross sections and isomeric yield ratios of the reaction $Re^{187}(d,p)-Re^{187m,g}$. The (n,γ) isomer ratio is from K. Takahashi, M. McKeown, and G. Scharff-Goldhaber, Phys. Rev. 136, B18 (1964).

performed individual bombardments with Van de Graaff deuterons of accurately known energies rather than computing the degradation of the beam through stacked targets, as was done in the present work.

The present Cd^{115} ratios, however, are in disagreement with those of Sharp and Pappas,⁸ as is shown in Fig. 5. Since these authors reported only the ratios and not the individual isomeric cross sections, the reason for the

¹⁸ D. C. Peaslee, Phys. Rev. 74, 1001 (1948).

disagreement is not easily found. The present results, however, are consistent with all other previously reported (d,p) isomer ratios in that they increase with increasing energy.

Although (d,p) isomer ratios are by their nature sensitive to structural details and are not susceptible to

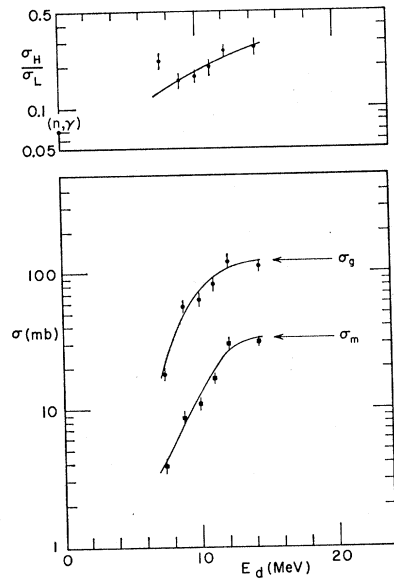


FIG. 9. Absolute cross sections and isomeric yield ratios of the reaction $Pt^{196}(d,p)-Pt^{197m,g}$. The (n,γ) isomer ratio is from M. L. Sehgal, Phys. Rev. 128, 761 (1962).

generalization, some rough correlations can be noted in the data. Figure 10 shows the measured isomer ratios at 14 MeV together with some previously determined (d,p) ratios, plotted against the difference in spin ΔI_H between the target and the high-spin isomer. As shown by the dashed line, there is a general decrease in the ratio as

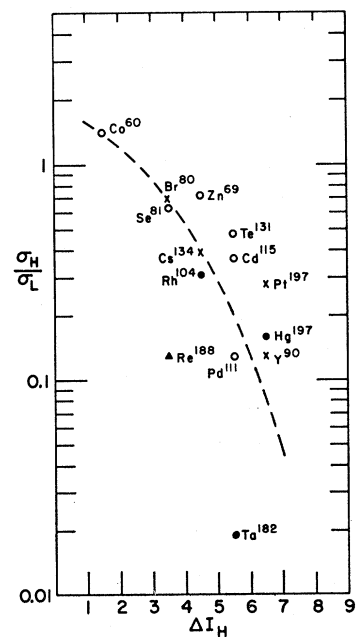


FIG. 10. Isomeric yield ratios of (d,p) reactions at 14 MeV as a function of ΔI_H , the spin difference between the target and the high-spin isomer. The numbers of known nuclear levels between the metastable and ground states are indicated by the plotting symbols: $\circ=0$, $\times=1$, $\bullet=2$, $\blacktriangle=3$. Ratios not measured in this work are from Refs. 6-10.

the amount of angular momentum needed to form the high-spin isomer increases. Superimposed on this trend is one which might be attributed to the existence of nuclear levels lying between the ground and metastable states of the residual nucleus. Since these can cascade only to ground, the ground-state cross section will be enhanced if such intermediate levels can be populated by the reaction. The isomer ratio σ_H/σ_L will thus be lowered if the ground state has the lower spin, as it does in all cases shown in Fig. 10 with the exception of Co⁶⁰. A general decrease in the isomer ratio with increasing number of known intermediate levels for the same ΔI_H is discernible in the figure.

B. (d,p) versus (n,γ) Isomer Ratios

One objective of the present work is to compare the isomer ratios from (d,p) reactions with those from thermal neutron capture in the same target, which leads to the same residual isomers. The known (n,γ) ratios have been plotted at zero energy in Figs. 1–9, where it can be seen that the (d,p) ratios extrapolate to values which are approximately equal to or somewhat larger than the (n,γ) ratios. This observation is reasonable in the light of certain similarities which have been noted between the two reactions. It has been observed,¹⁹ for example, that the primary gamma rays which are emitted following thermal neutron capture frequently correspond to transitions from the capturing state to the same lower-lying states which are populated in the (d,p) reaction. Furthermore, correlations between the intensities of some of these gamma rays and the intensities of (d,p) proton groups from the same targets have been observed. Lane and Wilkinson²⁰ point out that while the (n,γ) and (d,p) processes may be quite different in many respects, the matrix elements for the two reactions both contain a part which represents the parentage overlap between the initial and final states, and that this part of the matrix element can in some cases dominate. It has also been suggested²¹ that the intensity correlations can sometimes be attributed to a direct-capture mechanism for the (n,γ) reaction.

Whatever the explanation, the similarity observed in the present work between the (n,γ) and (d,p) isomer ratios at low energies may be another manifestation of the same gamma-ray-proton-group intensity correlation, for if the initially populated states are formed in the same relative abundances by neutron capture and by stripping, then the subsequent de-excitation gamma cascade will lead to the same value of the isomer ratios. Since even at low energies, however, the neutron deposited by the (d,p) reaction should carry some angular momentum into the residual system, the ultimate isomer ratio σ_H/σ_L might be expected to be somewhat

higher than that produced by the s -wave capture of the (n,γ) process.

IV. CALCULATIONS

A. Primary Spin Distributions

According to the distorted-wave Born-approximation (DWBA) theory of stripping,²² the differential cross section of a (d,p) reaction may be expressed as

$$\frac{d\sigma}{d\omega} = \frac{2J_f+1}{2J_i+1} \left(\frac{d\sigma}{d\omega} \right)_{\text{DWBA}} S(J), \quad (3)$$

where J_i and J_f are the total angular momenta of the initial and final states; $(d\sigma/d\omega)_{\text{DWBA}}$ is the differential cross section as calculated by DWBA theory and is a function of l_n , J , and Q ; and $S(J)$ is the spectroscopic factor for the (d,p) reaction, a measure of the emptiness of the target state. Integration over solid angle gives the total cross section for the insertion of a neutron into a single-particle state of total angular momentum J_f :

$$\sigma_{J_f} = \frac{2J_f+1}{2J_i+1} \sigma_{\text{DWBA}} S(J). \quad (4)$$

The cross section is thus calculated by multiplying the stripping-theory cross section σ_{DWBA} by terms, the values of which depend upon the structures of the initial and final nuclei.

According to the pairing theory of Kisslinger and Sorensen,^{23,24} E_j , the energy of the single-particle state j in an odd- A nucleus, is

$$E_j = [(\epsilon_j - \lambda)^2 + \Delta^2]^{1/2}, \quad (5)$$

where ϵ_j is the energy of the single-particle state in the absence of pairing interactions, Δ is the range of energy over which the shell-model states are mixed by the pairing interaction, and λ is the Fermi level. In the absence of pairing interactions, λ represents the level below which all states are filled and above which all states are empty. The emptiness of a particular state is given by

$$U_j^2 = 1 - \frac{1}{2} \left[1 - \frac{\epsilon_j - \lambda}{[(\epsilon_j - \lambda)^2 + \Delta^2]^{1/2}} \right], \quad (6)$$

where $U_j^2 = S(J)$ for the (d,p) reaction. The parameters ϵ_j , λ , and Δ have been tabulated for a number of nuclei.^{23,24}

In the present work, the calculation of the isomer ratios to be expected in (d,p) reactions is divided into two parts. First, the relative probabilities for the formation of product nuclei in different angular momentum states are determined. Then an estimation is made of

¹⁹ O. A. Wasson, K. J. Wetzal, and C. K. Bockelman, Phys. Rev. **136**, B1640 (1964).

²⁰ A. M. Lane and D. H. Wilkinson, Phys. Rev. **97**, 1199 (1955).

²¹ C. K. Bockelman, Nucl. Phys. **13**, 205 (1959).

²² N. K. Glendenning, Ann. Rev. Nucl. Sci. **13**, 191 (1963).

²³ L. S. Kisslinger and R. A. Sorensen, Kgl. Danske Videnskab. Selskab, Mat. Fys. Medd. **32**, No. 9 (1960).

²⁴ L. S. Kisslinger and R. A. Sorensen, Rev. Mod. Phys. **35**, 847 (1963).

the relative probabilities for the population of the two experimentally observed final states during the gamma-ray cascade which follows the capture of the neutron. As evidenced by Eq. (4), the first step requires certain structural information as well as DWBA calculations utilizing experimentally determined optical-model parameters. Unfortunately, however, the required information is available in relatively few cases. Furthermore, the extrapolation of the 15-MeV optical-model parameters to lower energies is difficult because their energy dependence in this range is not well understood.²⁵ The isomer-ratio calculations were limited, therefore, to those (d,p) reactions in even-even targets at 15 MeV for which the required data are available.

The method employed for determining the primary spin distributions in the product nuclei first requires that one choose the shell-model states which are expected to contribute to the total cross section for formation of the (d,p) product. For this purpose, the single-particle states with binding energies less than S_n , the separation energy of the last neutron in the product nucleus, were used; higher-energy states were assumed to be unstable to particle emission. The locations of the low-lying single-particle states were obtained from the (d,p) spectroscopic studies of Cohen and co-workers,²⁶ the calculations of Kisslinger and Sorensen,^{23,24} and the published level schemes.^{13,27} The spectroscopic factors $S(J)$ were obtained from the former two sources.

Since the higher-energy levels are unresolved in (d,p) studies and are not treated by the pairing-theory calculations, it was necessary to estimate the locations of those higher-energy single-particle states which might contribute to the total cross section of the reaction. These estimates were made by utilizing the single-particle neutron state data recently reviewed by Cohen.²⁶ Under the assumption that the metastable and ground states of the even-odd product nuclei contain 100% of the single-particle neutron states of the same angular momentum and parity, the excitation energy above which a single-particle state is unbound was taken as being equal to $[(B_m + B_g)/2] - S_n$, where B_m and B_g are the binding energies of the metastable and ground states, respectively, as obtained from Cohen's plot of binding energy versus mass number. Since the unresolved levels are either high in the filling shell and hence only sparsely populated or in the next higher shell, which is empty, the spectroscopic factors of these states were taken as unity. The total cross section for the reaction,

TABLE I. Calculated primary distribution of states in Cd^{115} from $\text{Cd}^{114}(d,p)$ at 15 MeV. The Cd and Sn data of Ref. 26 were employed.

| State | Q (MeV) | σ_{DWBA} (mb) | $S(J)$ | σ_J (mb) | $\sigma_{J, \text{rel}}$ |
|---------------|--------------|--------------------------------|--------|--------------------|--------------------------|
| $h_{9/2}$ | -2.3 | 1.7 | 1 | 17 | 0.086 |
| $p_{1/2}$ | -1.5 | 19.5 | 1 | 39 | 0.20 |
| $f_{5/2}$ | -0.9 | 4.7 | 1 | 28 | 0.14 |
| $p_{3/2}$ | 0.1 | 13.5 | 1 | 54 | 0.27 |
| $f_{7/2}$ | 1.1 | 3.1 | 1 | 25 | 0.13 |
| $d_{5/2}$ | 3.1 | 5.3 | 0.22 | 6.9 | 0.035 |
| $g_{7/2}$ | 3.4 | 0.63 | 0.15 | 0.76 | 0.004 |
| $d_{3/2}$ | 3.7 | 3.8 | 0.75 | 11 | 0.056 |
| $h_{11/2}(m)$ | 3.7 | 0.45 | 0.65 | 3.5 | 0.018 |
| $s_{1/2}(g)$ | 3.9 | 7.9 | 0.73 | 12 | 0.061 |

$\sigma_T = \sigma_m + \sigma_g$, is then the sum of the cross sections of the various contributing states:

$$\sigma_T = \sum_{\text{states}} \sigma_J.$$

In most cases the selection of higher levels from Cohen's plot of single-particle neutron binding energy versus A was unambiguous, and fairly good agreement was obtained between the calculated and experimental total cross sections. On the occasion that a state was found to be very close to the energy above which it should be excluded from the calculation as being unbound, the experimental total cross section was used as the criterion: Any such questionable state which increased the calculated total cross section significantly above the experimental value was excluded from the calculation.

The results of DWBA calculations²⁶ employing the code JULIE²⁸ were used to obtain σ_{DWBA} as a function of l_n , J , and Q . For each reaction, the cross section for the insertion of a neutron into each contributing single-particle state was calculated from Eq. (4). Table I shows the results of the calculation of the primary distribution of states in Cd^{115} . The relative cross section $\sigma_{J, \text{rel}}$ for each contributing state is σ_J/σ_T .

Although the U_j^2 values used for some of the lower-energy states were obtained primarily by a comparison of experimental differential cross sections with DWBA calculations, certain other experimental information²⁶ was generally included. The use of the resultant U_j^2 values, therefore, in most cases represents a more valid comparison of theory with experiment than would have been obtained by the somewhat circular process of regenerating the experimental data from DWBA theory through the use of U_j^2 values obtained by fitting the theory to experiment.

A recent evaluation²⁹ of the DWBA method indicates that in favorable cases the errors in U_j^2 are of the order of 20%. The relative error in the U_j^2 values for different states in the same nucleus, which are of primary interest

²⁵ C. M. Perey and F. G. Perey, Phys. Rev. **132**, 755 (1963).

²⁶ B. L. Cohen *et al.*, Rev. Mod. Phys. **35**, 332 (1963); B. L. Cohen, Phys. Rev. **130**, 227 (1963). For nuclides of interest in the present work see: (Zn) E. K. Lin and B. L. Cohen, Phys. Rev. **132**, 2632 (1963); (Se) E. K. Lin, *ibid.* **139**, 340 (1965); (Pd) B. Cujec, *ibid.* **131**, 735 (1963); (Cd) B. Rosner, *ibid.* **136**, B664 (1964); (Te) R. K. Jolly, *ibid.* **136**, B683 (1964); (Sn) E. J. Schneid, A. Prakash, and B. L. Cohen, *ibid.* (to be published) (1967). Data for the isotonic Sn isotopes were employed in choosing the spectroscopic factors for states in Pd^{111} and Cd^{115} .

²⁷ K. G. Prasad, K. P. Gopinathan, and M. C. Joshi, Nucl. Phys. **58**, 305 (1964).

²⁸ R. H. Bassel, R. M. Drisko, and G. R. Satchler, Oak Ridge National Laboratory Report No. ANL 3240 (unpublished).

²⁹ L. L. Lee, Jr., *et al.*, Phys. Rev. **136**, B971 (1964).

TABLE II. Calculated isomer ratios and effective moments of inertia for 15-MeV (d,p) reactions in even-even targets.

| Isomeric pair | Exptl. isomer ratio | R_m | Average multiplicity, $\sigma=3$ | | | | Individual multiplicities | | |
|--------------------------------------|---------------------|-------|----------------------------------|-------|-------|--|---------------------------|------------|--|
| | | | $M=3$ | $M=4$ | $M=5$ | $\mathcal{I}/\mathcal{I}_{\text{rigid}}$ | $\sigma=3$ | $\sigma=5$ | $\mathcal{I}/\mathcal{I}_{\text{rigid}}$ |
| Zn ⁶⁹ | 0.70 ^a | 0.60 | 0.72 | 0.81 | 0.90 | 0.81 | 0.45 | 0.76 | 2.5 |
| Se ⁸¹ | 0.62 ^b | 0.27 | 0.53 | 0.66 | 0.73 | 0.66 | 0.41 | 0.49 | ... |
| Pd ¹¹¹ | 0.15 ^c | 0.031 | 0.098 | 0.13 | 0.18 | 0.50 | 0.12 | 0.15 | 0.78 |
| Cd ¹¹⁵ | 0.38 ^c | 0.30 | 0.35 | 0.40 | 0.45 | 0.49 | 0.35 | 0.41 | 0.90 |
| Te ¹³¹ | 0.48 ^b | 0.38 | 0.40 | 0.42 | 0.44 | 0.63 | 0.32 | 0.44 | 1.6 |
| Pt ¹⁹⁷ | 0.30 ^d | 0.33 | 0.29 | 0.28 | 0.27 | 0.23 | 0.25 | 0.41 | 0.29 |
| Hg ¹⁹⁷ | 0.21 ^c | 0.30 | 0.28 | 0.27 | 0.26 | 0.14 | 0.26 | 0.37 | 0.17 |
| Average deviation from experiment, % | | ±36 | ±17 | ±14 | ±18 | | ±23 | ±24 | |

^a Reference 9.^b Reference 7.^c Present work.^d Reference 6.

in the present work, may be about 10%.³⁰ Since in all the calculations performed the bulk of the total cross section stemmed from the population of higher-energy unfilled states with spectroscopic factors of unity (see Table I for Cd¹¹⁵), the results were relatively insensitive to errors in U_j^2 .

B. Isomer Ratios by the Mean-Spin Approximation

A first approximation to the isomer ratio was made by assuming that each initially populated state having an angular momentum higher than the mean spin of the two isomeric states decays to the high-spin isomer, while each state having an angular momentum lower than the mean spin decays to the low-spin isomer. An initial state having angular momentum equal to the mean value was taken as feeding both isomers equally. In those cases in which nuclear levels are known to exist between the isomeric states, it was assumed that the metastable state competes with that intermediate level which is closest to it in spin.

The isomer ratios calculated in this way are designated R_m and appear in the third column of Table II, where they may be compared with the available experimental isomer ratios from (d,p) reactions on even-even targets at 15 MeV.³¹ In some of the cases presented, e.g., Zn⁶⁹ and Pt¹⁹⁷, R_m is a fair approximation to the experimental ratio. In other cases, notably Se⁸¹ and Pd¹¹¹, the agreement is poor.

C. Isomer Ratios by Gamma-Cascade Calculations

In order to make a more detailed calculation of the isomer ratio, one must account for the spin-fractionating gamma-ray cascade which follows capture of the neutron. Present knowledge of the nature of gamma cascades results primarily from the observation of neutron-capture gamma rays, where the multiplicity, or average number of steps in the gamma cascade, has been

found³² for a number of nuclei to be about 2 to 4. This value, however, represents only the more easily observed transitions and must be presumed to be only an approximation to the actual multiplicity. In the present calculations, the multiplicity of the cascade has been retained as a variable parameter.

The existing data on the multipolarity of gamma cascades indicate that dipole radiation predominates.³³ In the calculations described below, it has been assumed that the cascade consists entirely of $l=1$ photons except for the last step, in which one or both of the two competing final levels are populated. The fractionation into the observed isomeric states has been assumed to be governed only by the relative densities of the accessible nuclear levels.²⁻⁴ The relative level densities used are those given by statistical theory³⁴:

$$\rho(J) \propto (2J+1) \exp[-(J+\frac{1}{2})^2/2\sigma^2], \quad (7)$$

where σ is the spin cutoff parameter, which characterizes the angular momentum distribution of the levels.

Several theories^{35,36} have been used for the calculation of σ . In the Fermi gas model it is given by

$$\sigma^2 = cT = \mathcal{I}_{\text{rigid}} T / \hbar^2, \quad (8)$$

where T is the nuclear temperature, related to the excitation energy E by

$$E = aT^2 - T. \quad (9)$$

In the present calculations the level density parameter a was taken as $\frac{1}{8}A$.³⁷ The rigid-body moment of inertia $\mathcal{I}_{\text{rigid}}$ is given by

$$\mathcal{I}_{\text{rigid}} = \frac{2}{5}mAR^2, \quad (10)$$

where m is the nucleon mass, A is the mass number, and

³² C. O. Muehlhause, Phys. Rev. **79**, 277 (1950); L. V. Groshev *et al.*, At. Energ. **4**, 5 (1958).

³³ A. G. W. Cameron, Can. J. Phys. **35**, 666 (1957); V. M. Strutinski, L. V. Groshev, and M. K. Akimova, Nucl. Phys. **16**, 657 (1960); B. B. Kinsey and G. A. Bartholomew, Phys. Rev. **101**, 1328 (1956); J. M. Mollenauer, *ibid.* **127**, 867 (1962).

³⁴ C. Bloch, Phys. Rev. **93**, 1094 (1954).

³⁵ T. Ericson, Advan. Phys. **9**, 425 (1960).

³⁶ D. W. Lang, Nucl. Phys. **42**, 353 (1963).

³⁷ J. M. B. Lang and K. J. LeCouteur, Nucl. Phys. **13**, 32 (1959).

³⁰ R. M. Drisko (private communication).

³¹ For the purposes of these comparisons, the 15-MeV ratios were obtained by making short energy extrapolations. The extrapolation of the 11-MeV Hg¹⁹⁷ ratio was made by assuming that it has the same energy dependence as the Pt¹⁹⁷ ratio.

R is the nuclear radius, taken in the present calculations as $1.2A^{1/3}$ F.

It has been assumed in the present calculations that both the gamma cascades and the spin distributions of nuclear levels are similar in the (d, p) and (n, γ) reactions in the same targets. In view of the similarities which have been pointed out in Sec. III B, the assumption that the cascade which follows (d, p) stripping is essentially the same as that which follows neutron capture is not unreasonable, although the multiplicity might be expected to be lower in the (d, p) reactions because of the lower average excitation energies involved.

The validity of statistical-theory predictions for the relative densities of levels of different angular momenta is open to some question at the low excitation energies encountered in (d, p) reactions. Since statistical-theory relative level densities have been employed successfully in the calculation of (n, γ) isomer ratios,² however, and in view of the presumed similarity of the (d, p) and (n, γ) cascades, the use of the same formulation for relative level densities in the (d, p) and (n, γ) reactions is not unreasonable.

Average multiplicity. In a compound-nucleus reaction, the capture of projectiles of a given energy produces compound nuclei having the same excitation energy, but a variety of angular momenta. These compound nuclei then de-excite by particle and photon emission to form the product nuclei. Since the initial energies of all the compound nuclei are the same, the number of steps in the spin-changing gamma de-excitation process is probably well represented by some average value. In direct interactions, on the other hand, the "centers of gravity" of the shell-model states of different angular momenta usually lie at quite different excitation energies. Thus the numbers of steps in the gamma cascades from different states undoubtedly differ significantly. The isomer ratios of this section have nevertheless been calculated by applying an average multiplicity to the decay of all states formed. That is, it was assumed that a state of angular momentum J_1 at high excitation energy de-excites in the same number of steps as a state of angular momentum J_2 at low excitation energy.

Account was taken of the spin redistribution resulting from the gamma cascade by using the DWBA primary spin distributions as input data in the third part of Vandenbosch and Huizenga's computer program,³⁸ by which the distributions resulting from successive gamma-ray emission are calculated on the assumption that Eq. (7) applies. Not all of the quasiparticle states were considered to be involved in the spin-fractionating cascade. States lying between the metastable and ground states, for example, can cascade only to ground. Furthermore, on the assumption that the metastable and ground states of even-odd nuclei contain 100% of the single-particle neutron states of the same J and π , only those

³⁸ W. L. Hafner, Jr., J. R. Huizenga, and R. Vandenbosch, Argonne National Laboratory Report No. ANL 6662 (unpublished).

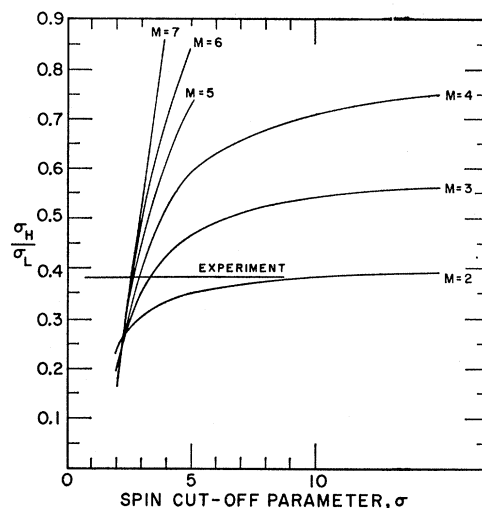


FIG. 11. The $\text{Cd}^{114}(d, p)\text{Cd}^{115m, s}$ isomeric yield ratio at 15 MeV, calculated for different γ -ray multiplicities M and spin cutoff parameters σ , according to the methods described in Sec. IV of the text.

states lying above the metastable state were treated in the calculation.

For various combinations of multiplicity M and spin cutoff parameter σ , the isomer ratios were calculated in a manner similar to that described in Sec. IV B. That is, the cascade was cut off at a value of angular momentum half-way between the spins of the two competing final levels. All states with residual angular momenta above this value were then permitted to emit one more photon to reach the high-spin isomeric state; all states with residual angular momenta below the cutoff value were permitted to emit one more photon to reach the low-spin isomer. Any level of angular momentum equal to the cutoff value was assumed to populate the two levels equally.

In Fig. 11, the calculated ratios for Cd^{115} are shown as a function of σ for different multiplicities. The intersections of the experimental ratio (horizontal line) with the curves for different multiplicities represent different combinations of the two variables which are capable of reproducing the experimental results. For $M > 3$, the value of σ which is required for agreement with experiment changes slowly. Similar results were obtained for each isomeric pair for which an isomer ratio was calculated. The best agreement with experiment was obtained by setting $\sigma = 3$ and $M = 3, 4, \text{ or } 5$. In the fourth, fifth, and sixth columns of Table II, the isomer ratios obtained by using these values of the parameters are compared with experiment. Note that in those cases in which R_m was a good approximation to the experimental ratio, relatively little change has been made by including the gamma cascade. On the other hand, where R_m was not a good approximation, the ratio obtained by including the gamma cascade is significantly closer to the experimental ratio. There is, of course, no reason to expect either σ or M to be the same in all nuclei. Thus,

for $\sigma=3$, the value $M=3$ gives the best prediction for Zn^{69} , while $M=5$ is best for Te^{131} . The best over-all agreement, however, is given by $\sigma=3$ and $M=4$; these values of the parameters reproduce the seven experimental isomer ratios in Table II with an average deviation of 14%.

Individual multiplicities. An attempt was made to allow for different numbers of steps in the gamma-ray cascades from different states. The mean energy of a dipole gamma ray emitted from a nucleus of excitation energy E was taken as³

$$\bar{E}_\gamma = 4[(E/a) - (5/a^2)]^{1/2}, \quad (11)$$

where E is the excitation energy of the nucleus before gamma-ray emission and a is the nuclear level density parameter. Starting with $E=E_j$, the mean energy of the first gamma ray was calculated; the energy of each successive gamma ray was then obtained by using the average excitation energy remaining after the emission of the preceding one. To determine the excitation energy at which the final transition occurs, leading either to the metastable or to the ground state, the procedure of Bishop *et al.*³ was employed. That is, it was assumed that a transition leaving a residual excitation energy of less than 1 MeV will be followed by the final gamma ray, which populates one of the two isomeric states. If the residual excitation energy is more than 2 MeV, the next gamma ray will not be the final one. When a transition leaves the nucleus with an excitation energy between 1 and 2 MeV, the probability that the final gamma ray will be preceded by another one is taken as $E-1$.

In this way, individual multiplicities were arrived at for each initially populated single-particle state. The eighth and ninth columns of Table II show the resultant isomer ratios, calculated for $\sigma=3$ and $\sigma=5$. The average deviations show that allowance for individual multiplicities offers no advantage over the use of an average multiplicity for all states. Both types of cascade calculations, however, give substantially better agreement with experiment than does the mean-spin approximation.

Effective moments of inertia. The value of the spin cutoff parameter which produces the best agreement between the cascade calculations and experiment can be expressed as an effective nuclear moment of inertia through a relation of the form of Eq. (8). In the average multiplicity calculations, since the value of σ which is required to produce agreement with experiment changes slowly above $M=3$, the moments of inertia were obtained from the average values of σ for multiplicities of 3, 4, 5, and 6. The results are expressed in the seventh column of Table II as fractions of the rigid-body moments of inertia at $T=0.5$ MeV, the average temperature of the (d,p) product nuclei. A general decrease in $\mathcal{I}/\mathcal{I}_{\text{rigid}}$ with increasing nuclear mass is noted.

In the individual multiplicity calculations, it was possible in each case to extract a unique value of the spin cutoff parameter which gave the best agreement with the experimental ratios. The corresponding effective

moments of inertia appear in the last column of Table II. Although a tendency of $\mathcal{I}/\mathcal{I}_{\text{rigid}}$ to decrease with increasing mass can be observed, unsuitably high values are obtained for Zn^{69} and Te^{131} . These are probably a result of the failure of statistical assumptions when applied to the detailed properties of nuclei at low excitation energies.

V. SUMMARY

The nine (d,p) isomer ratios measured in the present work are qualitatively similar and are consistent with a direct-reaction mechanism in which relatively little angular momentum is imparted to the target nucleus.

For (d,p) reactions in even-even targets at 15 MeV, calculations of the isomer ratios by using DWBA cross sections and allowing for spin redistribution during a subsequent gamma cascade lead to good agreement with experiment when the spin cutoff parameter is taken as 3 and the cascade multiplicity is taken as 4. For multiplicities of 3 to 6, the average value of the spin cutoff parameter which is required to produce agreement between the calculated and experimental ratios leads to values of $\mathcal{I}/\mathcal{I}_{\text{rigid}}$ which decrease with increasing mass number in agreement with previously reported data.^{39,40}

Attempts to refine the calculation by using a different multiplicity for the cascade from each contributing state result in poorer agreement with the experimental isomer ratios and in values of $\mathcal{I}/\mathcal{I}_{\text{rigid}}$ having less internal consistency.

ACKNOWLEDGMENTS

The authors wish to thank B. L. Cohen, F. W. Pement, and E. J. Schneid for helpful discussions; R. M. Drisko, W. L. Hafner, and P. Crowley for making their computer programs available; and the operators of the University of Pittsburgh Cyclotron for providing deuterons. One of us (J. B. N.) gratefully acknowledges fellowship assistance from the National Science Foundation and the National Aeronautics and Space Administration. Calculations were performed at the University of Pittsburgh Computation Center, which is partially supported by the National Science Foundation.

APPENDIX: EXPERIMENTAL DETAILS

$\text{Co}^{60m,g}$. The targets were 99.9% Co foils, 12.3 mg/cm² thick. Immediately after the irradiation, the 10.5-min, 59-keV isomeric transition ($\alpha_T=47$) was observed by scintillation counting. The foils were then dissolved in HCl, and Co was separated from Fe by elution from Dowex 1 resin. Cobalt was precipitated as $\text{Co}(\text{OH})_2$, then as $\text{CoNH}_4\text{PO}_4 \cdot \text{H}_2\text{O}$.⁴¹ The Co^{60g} disintegration rate

³⁹ J. H. Carver, G. E. Coote, and T. Sherwood, Nucl. Phys. 37, 449 (1962).

⁴⁰ R. Vandenbosch, L. Haskin, and J. C. Norman, Phys. Rev. 137, B1134 (1965).

⁴¹ H. D. Dakin, Z. Anal. Chem. 39, 789 (1900).

was determined by counting the 1.17- and 1.33-MeV gamma rays.

$Y^{90m,g}$. Powder targets⁴² of 99.99% Y_2O_3 , ranging in thickness from 5 to 15 mg/cm², were irradiated. Yttrium was precipitated as YF_3 and $Y(OH)_3$, then extracted from HNO_3 solution into *t*-butyl phosphate+Gulf Oil Company solvent BT.¹³ After precipitation of $Y(OH)_3$, a final precipitate of $Y_2(C_2O_4)_3 \cdot 10H_2O$ was vacuum dried. The 3.2-h metastable-state activity was determined by counting the 0.202-MeV ($\alpha_T=0.09$) transition.⁴² The 64-h ground-state activity was obtained by counting the 2.27-MeV β^- .

$Rh^{104m,g}$. Two sets of irradiations were performed. First, high purity Rh foils, 5.54 mg/cm² thick, were irradiated. Immediately after the irradiation, the foils were covered with 300-mg/cm² Al absorbers and the 42-sec ground-state activity was determined with a Geiger counter and a strip-chart recorder on fast drive. The isomer ratio was then calculated from the transient equilibrium relationship between the metastable and ground states.⁴³ In a second set of experiments, the same target foils were again irradiated and the activity of the 4.4-min metastable state was determined by absolute β counting. The ground-state cross sections were then calculated from the metastable-state activities and the isomer ratios of the first set of irradiations.

$Pd^{111m,g}$. The targets were high-purity Pd foils, 7.79 mg/cm² thick. Palladium was precipitated as the dimethyl glyoximate (DMG). The precipitate was then dissolved in conc. HNO_3 . Following two $Fe(OH)_3$ scavenges and two AgI precipitations, $Pd(DMG)_2$ was reprecipitated. The cross section for production of the 22-min ground state and the isomer ratio calculated therefrom by using the transient equilibrium equations were determined from the β activity measured through a 550-mg/cm² Al absorber. The cross section for production of the 5.5-h metastable state was also determined independently by counting the 0.16-MeV gamma ray.⁴⁴

$Cd^{115m,g}$. Enriched CdO powder targets, 98.53% Cd^{114} , were irradiated and dissolved in HCl to which standard Cd carrier had been added. Following three cycles of CdS precipitation, $FeOH(C_2H_3O_2)_2$ scavenging, and

AgCl scavenging, $CdNH_4PO_4 \cdot H_2O$ was precipitated, dried, and mounted. The activities of both Cd isomers were determined by β counting. Empirical self-absorption curves were used. The measured cross sections were corrected for a small contribution from the $Cd^{116}(d,t)$ - Cd^{115} reaction by comparing the results of the enriched target irradiations with the cross sections obtained by irradiating natural Cd foils.

$Cs^{134m,g}$. Following the irradiations, the CsCl powder targets were dissolved in hot H_2O . Two $Fe(OH)_3$ scavenges, a $BaCO_3$ precipitation, and two $La(OH)_3$ scavenges were followed by the precipitation of $Cs_3Bi_2I_9$. This precipitate was dissolved, I_2 was driven off by heating, and $Cs_3Bi_2I_9$ was again precipitated. The metastable-state activity was determined from the 127-keV isomeric transition; the ground-state activity was determined by counting the 800-keV γ rays.⁴⁵

$Ta^{182m,g}$. No chemical separations were performed. The irradiated high-purity Ta foils were mounted for counting immediately after the irradiation. The 16-min metastable-state activity was determined from measurements of the 56-keV *K* x ray accompanying 88% of the disintegrations.¹⁷ The 115-day ground state activity was determined by counting the 1- to 1.3-MeV gamma rays.

$Re^{188m,g}$. The targets, of 99.99% pure Re metal, were dissolved in hot $HNO_3-H_2O_2$ solution. Re was separated by pyridine extraction from basic solution and precipitated as Re_2S_7 , which was then dissolved in $HNO_3-H_2O_2$. Following $Fe(OH)_3$ scavenges, tetraphenylarsonium perrhenate was precipitated and mounted for counting. The 18.5-min Re^{188m} activity was measured by counting the ~ 80 -keV photons which accompany 89% of the disintegrations.⁴⁶ The 2.1-MeV β activity of the ground state was used to calculate σ_g .

$Pt^{197m,g}$. Powdered metal targets, enriched to 45.76% in Pt^{196} , were dissolved in aqua regia containing standardized Pt carrier. Gold was extracted into ethyl acetate. Platinum was extracted into ethyl acetate after reduction with $SnCl_2$ to $PtCl_4^-$. Platinum metal was then precipitated by reduction in HCl solution with Mg powder. The 20-h ground-state β activity and the 0.346-MeV γ activity of the 86-min metastable state²⁷ were measured.

⁴² J. M. Ferguson, Nucl. Phys. **27**, 334 (1961); C. Carter-Waschek and B. Linder, *ibid.* **27**, 1415 (1961).

⁴³ R. C. Greenwood, Phys. Rev. **129**, 339 (1963).

⁴⁴ V. R. Pandharipande, R. M. Singru, and R. P. Sharma, Phys. Rev. **140**, B1488 (1965).

⁴⁵ R. A. Brown and G. T. Ewan, Bull. Am. Phys. Soc. **10**, 82 (1965).

⁴⁶ S. B. Burson *et al.*, Phys. Rev. **136**, B1 (1964).